IEEE Access
Multidisciplinary | Rapid Review | Open Access Journal

Received February 6, 2021, accepted February 22, 2021, date of publication March 4, 2021, date of current version March 16, 2021.

Digital Object Identifier 10.1109/ACCESS.2021.3063836

Enhanced Target Ship Tracking With Geometric Parameter Estimation for Unmanned Surface Vehicles

JUNGWOOK HAN[1], SUN YOUNG KIM[1], AND JINWHAN KIM[2], (Member, IEEE)

[1]Autonomous & Intelligent Maritime Systems Research Division (AIMS), Korea Research Institute of Ships and Ocean Engineering (KRISO), Daejeon 34103, South Korea

[2]Department of Mechanical Engineering, Korea Advanced Institute of Science and Technology (KAIST), Daejeon 34141, South Korea

Corresponding author: Jungwook Han (jungwook@kriso.re.kr)

This work was supported in part by the Unmanned Vehicles Core Technology Research and Development Program through the National Research Foundation of Korea (NRF) and Unmanned Vehicle Advanced Research Center (UVARC) funded by the Ministry of Science and ICT, the Republic of Korea (Development of unmanned surface vehicle for autonomous cooperation) under Grant NRF-2020M3C1C1A02086423, and in part by the Promotion of Innovative Businesses for Regulation-Free Special Zones funded by the Ministry of SMEs and Startups (MSS), South Korea (Demonstration of Unmanned Surface Vehicle for a Maritime Survey) under Grant P0012448.

ABSTRACT Autonomous collision detection and avoidance is a crucial requirement for the safe navigation of unmanned surface vehicles (USVs) in maritime traffic situations. Automatic identification system (AIS) is used to obtain the motion information of surrounding ships and their dimensional specifications. With AIS information, appropriate collision risk assessment between two ships can be performed; further, collision avoidance can be achieved by defining a safe radius of avoidance, which can be determined considering the shape parameters of a target ship. However, AIS data are often unreliable and some commercial fishing vessels intentionally turn off the public tracking system to hide their location. Under these circumstances, marine radars are used to detect and estimate the motion information of nearby ships. However, most existing target tracking studies model the target as a point object without any spatial extent, and thus, its physical dimensions cannot be identified. In this paper, a target tracking method that uses a marine radar is proposed to simultaneously estimate the motion states (i.e., position, course, and speed) of a target ship and its geometric parameter (length) in the framework of an extended Kalman filter (EKF). The proposed approach enhances collision avoidance by providing the kinematic and length parameters to evaluate collision risk and generate an appropriate collision-free path. Real-sea experiments using a developed USV system were conducted to verify and demonstrate the feasibility of the proposed algorithm; the results are presented and discussed in this paper.

INDEX TERMS Geometric parameter estimation, marine radar, target motion analysis, unmanned surface vehicle.

I. INTRODUCTION

Over several decades, autonomous navigation technologies for unmanned surface vehicles (USVs) have advanced owing to the development of sensing and computing capabilities [1]. Autonomous collision detection and avoidance is a crucial requirement in these navigation technologies for the safe operation of USVs in maritime traffic environments.

The associate editor coordinating the review of this manuscript and approving it for publication was Rui-Jun Yan.

For collision detection, information about the surrounding ships including position, course, and speed is obtained using maritime navigation aid systems such as automatic identification system (AIS), electronic chart display and information system (ECDIS), and automatic radar plotting aid (ARPA). The collision risk is then evaluated using the collected information.

The shape parameters (i.e., length and breadth) of a nearby target ship involved in the collision are required for the accurate estimation of the collision risk [2]. For an analytical formulation of collision risk assessment, a circular boundary

is employed; its radius is determined based on the obtained shape parameters [2], [3]. The parameters are also required to generate an appropriate collision-free path to achieve automatic collision avoidance with a target ship that has a high collision risk. In particular, a safe (or minimum) radius of avoidance is defined considering the length of traffic ships involved in the collision, and evasive routes are generated for the USV to ensure safe navigation in maritime traffic situations.

AIS plays an important role in maritime traffic safety as it provides the motion information of traffic ships along with specifications such as length, breadth, and ship type. Thus, appropriate collision avoidance can be achieved by accurately assessing the collision risk and defining the safe radius of avoidance.

However, AIS is often unreliable and reports incorrect ship information in many cases [4]; further, some commercial fishing vessels intentionally turn off the public tracking system as fishers do not want to reveal their fishing location to other vessels [5]. Under these circumstances, marine radars are used to detect and estimate the motion information of the surrounding ships. Most existing target tracking studies model the target as a point object without any spatial extent, and therefore, physical dimensions cannot be identified.

Shape parameters are crucial to ensure the navigational safety of a USV when the vehicle approaches a target ship in a crossing scenario. When AIS data are not available, the conventional ARPA system estimates the motion of target ship based on the time-varying trajectory obtained using consecutive radar images; then, collision-free path is generated considering an arbitrarily defined safe radius of avoidance. By setting the safe radius to a large value, the USV can conservatively avoid an approaching target ship whose shape parameters are unknown. However, this approach does not provide an accurate evaluation of ship collision or support the generation of an efficient collision-free path. In addition, this approach can lead to ship collisions even if appropriate collision risk assessment is performed between two ships because routes created for collision avoidance can overlap the region occupied by a large-sized target ship. Therefore, safe vehicle navigation requires not only kinematic parameters of the target ship, but also its geometric parameter.

In this paper, a target tracking algorithm is introduced to estimate the motion of the target ship with a marine radar mounted on a USV. An enhanced target ship tracking approach is proposed in this study, wherein the geometric and kinematic parameters of a target are estimated simultaneously. When a USV encounters a target ship whose geometric parameters are not available a priori, the proposed method enhances its collision avoidance capability by providing shape information to evaluate the ship collision risk accurately and to generate an appropriate collision-free path.

The remainder of this paper consists as follows: Section II introduces and discusses related work on modern target tracking. The proposed target tracking algorithm is introduced in Section III. Section IV demonstrates and validates the method via real-sea experiments. Finally, conclusions are presented in Section V.

II. RELATED WORK

There are several studies that focus on target tracking using various types of detection sensors such as lidars, cameras, sonars, and radars [6]–[11].

In ground vehicle applications, lidar and camera sensors were used to detect and track relatively small objects such as pedestrians and cars by describing them as point objects [12], [13]. Also, short-range radars were used for self-driving cars as a moving objects tracker (MOT) subsystem.

In marine vehicle applications, sonars were employed to estimate the motion of underwater targets within the framework of bearing-only target motion analysis (BOTMA) [14], [15]. To describe the motion of targets in BOTMA, a constant velocity (CV) model was used for tracking targets in a nominal speed [14]; interacting multiple model (IMM) was used for tracking maneuvering targets [16]. Further, marine radars were used as the main sensor for target ship tracking as they are robust against various weather conditions and provide the relative position information of surrounding traffic ships over a wide area [17]–[20].

Most existing target tracking studies consider the target as a point object; kinematics parameters such as position, course, and speed are estimated within the framework of target motion analysis (TMA). However, with the advancement of sensing technology, sensor signals reflected from target surfaces occupy several sensor resolution cells, and thus the shape of the target could be also estimated in the tracking filter, which is known as extended target tracking (ETT) or extended object tracking (EOT).

After the initial research on ETT [21], [22], considerable research was conducted to track moving objects such as cars, bicyclists, ships and humans [21]–[25]. In these cases, the shape and size of the objects did not change over time, and thus extent states could be estimated with the kinematic parameters using the ETT algorithm. Specific geometric primitives such as sticks, circles, rectangles, and ellipses were employed; their shape parameters were estimated with their motion states in the tracking filter. For example, two-dimensional (2D) lidar measurements were used to detect bicycles and cars, and they were represented by sticks and rectangles, respectively [26]–[28].

Recently, research studies employed an ellipse primitive to track maritime traffic ships with radar sensors [17], [19], [20]. Since X-band marine radars provide reasonable measurement resolutions, they are commonly used for target ship detection and tracking in navigational assistance systems. A joint probabilistic data association (JPDA)-based ETT was conducted by involving ellipse parameters obtained from a high-resolution X-band radar fixed on the ground for port surveillance in the Gulf of La Spezia, Italy [23]. The ellipse parameters were defined according to the two lengths of the major and minor axes and their orientation, which were

obtained by fitting radar measurements reflected from the target; the target orientation was assumed to be identical to the orientation of the extracted ellipse. However, this assumption may not be applicable unless the radar reflections do cover the entire surface of the target. For example, the radar mounted on a small- or mid- size USV can provide partial measurements depending on the relative horizontal and vertical positions between the USV and the target.

In this paper, an enhanced target ship tracking approach is proposed to estimate both the motion states and geometric parameters of the target by extending the authors' previous work [10], [29], wherein traditional target tracking was conducted considering a target detected via radar measurements as a point object. Unlike previous studies on ETT wherein a specific model is assumed to extract the orientation (i.e., heading) of a target ship by fitting radar measurements, our approach does not assume a specific model and extracts the length of the target ship by associating the course estimated in the tracking filter and radar measurements reflected from a partial surface of the target. The proposed method enhances the safe navigation of USVs in maritime traffic scenarios by providing both kinematic states and length parameter to detect collision risks and generate collision-free paths.

III. PROBLEM FORMULATION

A common target detection and motion estimation approach is to extract the center positions of targets on a radar image, and then to estimate their motion including position, course, and speed from time-varying position coordinates. In this study, the length of a target ship is also considered and the value is estimated with her motion states. The proposed approach could enhance safe collision avoidance by providing the geometric information to generate a collision-free path.

A. TARGET DETECTION AND GEOMETRIC PARAMETER EXTRACTION

A radar image is generated from radar measurements and several blobs on the image are occupied by reflections from a target. A single blob is defined by the range and bearing resolutions; hereafter, it is also referred to as a cell.

A set of preprocessing steps is necessary to extract targets from the radar image, including both real targets and unwanted echoes (i.e., clutter) [10]. To this end, fast time constant (FTC) and sensitivity time control (STC) are applied to minimize clutter returns from the rain and the water surface. Areas reflected from marine infrastructures and landmass are eliminated by assigning a region of interest (ROI) on the radar image.

A dynamic thresholding approach is employed to extract target blobs on the preprocessed radar image. In this study, a cell averaging constant false alarm rate (CA-CFAR) detector is applied by defining a window mask whose size is determined considering the size of targets of interest; then, the extracted blobs are classified into an identical target [30], [31]. The introduced target detection procedure is illustrated by the examples in Fig. 1.

From the obtained and classified cells, the center point is extracted and its position is estimated from the relative bearing and range information. Because radar images are generated by representing a stream of radar spokes considering range and bearing resolutions, the bounding box including target reflections can be described using a fan-shaped polygon as shown in Fig. 2(a).

In the bounding box, the occupied cells differ depending on the course of the target in the body-fixed frame. Therefore, an approximate measurement of the geometric parameter of the target can be obtained from the intersection points between the boundary of the polygon and the line that passes the center position at the angle of the course as shown in Fig. 2(b). In this study, the target orientation (i.e., heading) and its motion orientation (i.e., course) are assumed to be identical considering that the difference between heading and course angles is negligible when ships operate in conventional maritime traffic scenarios with a nominal speed.

B. ENHANCED TARGET TRACKING

To estimate the target motion with time-varying relative position measurements obtained from radar images, an extended Kalman filter (EKF) is applied with a continuous white noise acceleration model [8]. An enhanced target tracking method is formulated and applied to estimate the geometric parameter of a target and the motion states of the vehicle simultaneously. The length of the target is incorporated as a geometric parameter in the proposed tracking filter as it is the main shape information used for evaluating ship collision risk and for generating collision-free paths.

1) SYSTEM MODEL

To describe the motion of a USV and a target ship, a kinematic model with three-degrees-of-freedom (3 DOF) is applied assuming that the two vehicles move in a horizontal plane. The state vector of the USV is expressed as

$$\mathbf{x}_{\mathrm{U}} = [\, x_{\mathrm{U}} \;\; y_{\mathrm{U}} \;\; \psi_{\mathrm{U}} \;\; V_{\mathrm{U}} \,]^{\top} \tag{1}$$

where x_{U} and y_{U} are the position coordinates defined in the global frame, ψ_{U} is the heading, and V_{U} is the longitudinal speed. The equation of the vehicle's motion is given as

$$\dot{\mathbf{x}}_{\mathrm{U}} = [\, V_{\mathrm{U}} \cos\psi_{\mathrm{U}} \;\; V_{\mathrm{U}} \sin\psi_{\mathrm{U}} \;\; 0 \;\; 0 \,]^{\top}. \tag{2}$$

To estimate the motions of the USV and targets simultaneously, the augmented state vector is described by cascading the USV state vector $\mathbf{x}_{\mathrm{U}}$ and the target state vector $\mathbf{x}_{\mathrm{T}}$. The state vector of the i^{th} target can be written as

$$\mathbf{x}_{\mathrm{T}_i} = [\, x_{\mathrm{T}_i} \; y_{\mathrm{T}_i} \; \psi_{\mathrm{T}_i} \; V_{\mathrm{T}_i} \; l_{\mathrm{T}_i} \,]^{\top} \tag{3}$$

where x_{T_i} and y_{T_i} are the position coordinates defined in the global frame, ψ_{T_i} is the course, V_{T_i} is the longitudinal speed, and l_{T_i} is the geometric parameter (i.e., length). The equation of the i^{th} target motion can be written as

$$\dot{\mathbf{x}}_{\mathrm{T}_i} = [\, V_{\mathrm{T}_i} \cos\psi_{\mathrm{T}_i} \;\; V_{\mathrm{T}_i} \sin\psi_{\mathrm{T}_i} \;\; 0 \;\; 0 \;\; 0 \,]^{\top}. \tag{4}$$

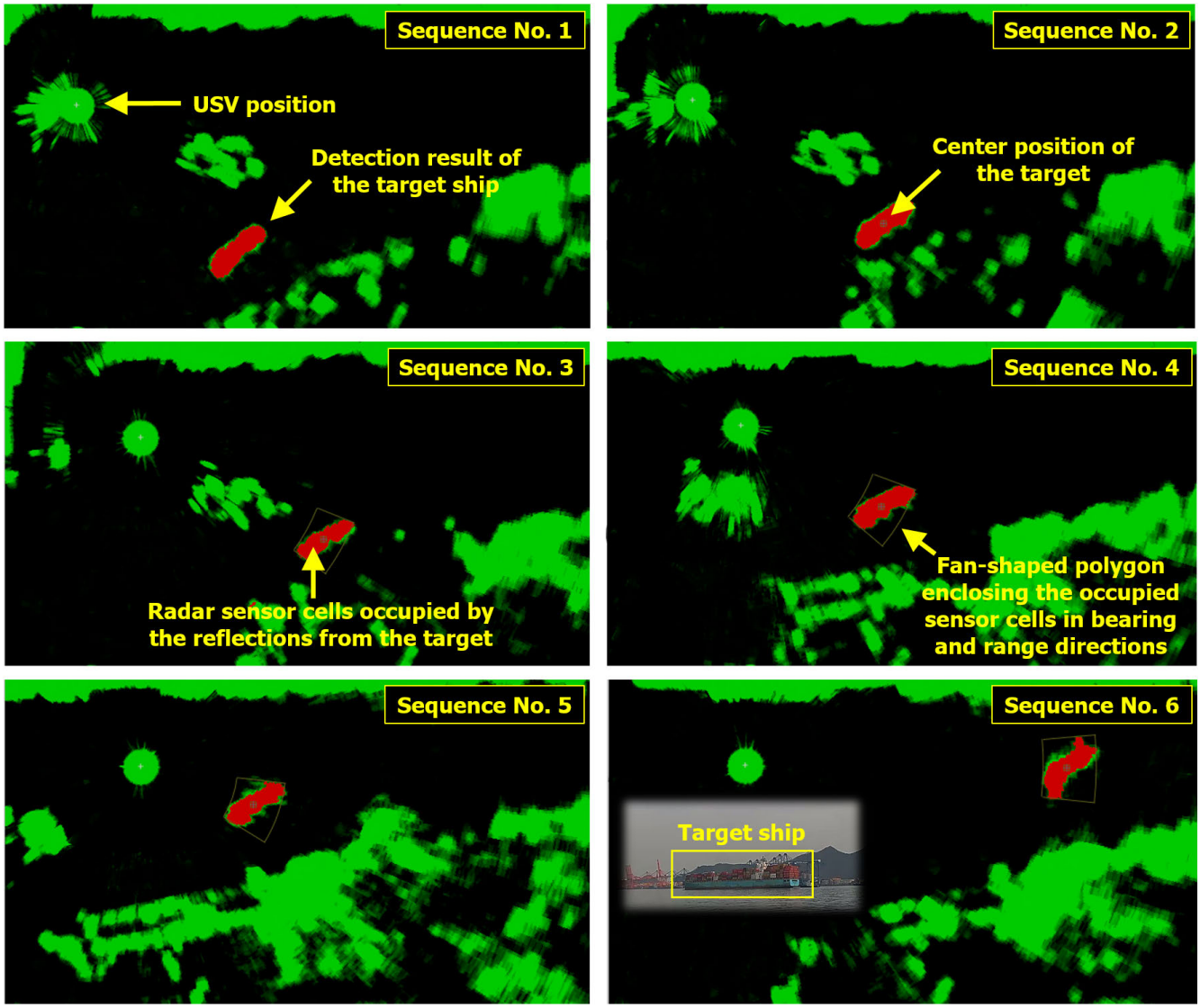

FIGURE 1. Sequence of target detection results from radar measurements. Raw radar signals are described with green blobs (or cells) and the radar signals reflected from the target are described with red blobs. A single blob represents a sensor cell defined by the range and bearing resolution of the radar. The fan-shaped polygon represents the boundary including all the occupied sensor cells (i.e., radar signals reflected from target); the polygon shape is described by the distances of the cells in the range and the bearing directions of the radar. The radar may not detect all surfaces of the target ship; partial reflections are obtained per scan, and the shape of the radar reflections changes slightly depending on the relative position between the USV and the target ship.

Multiple target tracking can be performed in this formulation, and thus the entire dimension of the target state vector is extended by the number of registered targets. The equation of the system dynamics involving the augmented state vector is expressed as

$$\dot{\mathbf{x}} = [\ \dot{x}_{\mathrm{U}}^{\top}\ \ \dot{x}_{\mathrm{T}_1}^{\top}\ \ \dot{x}_{\mathrm{T}_2}^{\top}\ \ \cdots\ ]^{\top} + \mathbf{w} \tag{5}$$

where $\mathbf{w}$ is the zero-mean Gaussian process noise employed to reflect the uncertainty in the system.

2) MEASUREMENT MODEL

To update the motions of the USV and the target, two sets of measurements are employed. The estimated motion of the USV is corrected by the first measurement dataset $\mathbf{z}_{\mathrm{U}}$, which is provided by onboard navigation sensors such as global positioning system (GPS), compass, and inertial measurement unit (IMU). The equation of the first measurement dataset is expressed as

$$\mathbf{z}_{\mathrm{U}} = [\ z_x\ z_y\ z_\psi\ z_V\ ]^{\top} = [\ x_{\mathrm{U}}\ y_{\mathrm{U}}\ \psi_{\mathrm{U}}\ V_{\mathrm{U}}\ ]^{\top} + \mathbf{v}_{\mathrm{U}} \tag{6}$$

where z_x and z_y represent the position measurements defined in north and east directions of Universal Transverse Mercator (UTM) coordinates, z_ψ represent heading measurement, and z_V represent speed measurement, which are provided by the navigation sensors. Further, $\mathbf{v}_{\mathrm{U}}$ is the zero-mean Gaussian noise employed to reflect the uncertainty in the measurement model.

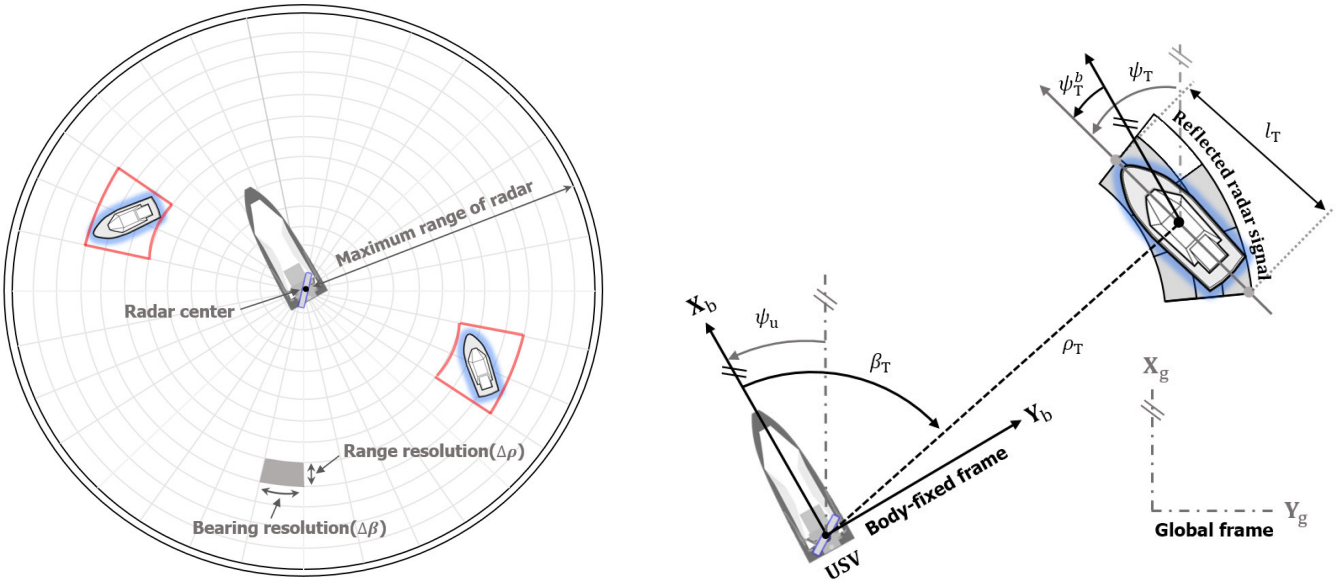

(a) Illustration of the radar sensing mechanism

(b) Coordinate system

FIGURE 2. Coordinate systems for target parameterization with radar sensor measurements. (a) A radar image is created considering signals and sensor resolution in the bearing and range directions. A single cell (shaded gray area) on the radar image is defined by the resolution characteristics. Multiple detections per target are obtained from radar measurements, and therefore, multiple cells are occupied by a single target on the radar image. A fan-shape polygon (solid line in red) is defined by the endpoints of the occupied cells in the range and bearing directions. (b) The position coordinates of the center of the target are defined by the relative range (ρ_{T}) and bearing (β_{T}) information. The target length l_{T} can be obtained by associating the course of the target (ψ_{T}^{b}) and the boundary of the fan-shape polygon including multiple cells occupied by the target's reflections. In the coordinates, clockwise represents positive direction.

The estimated motion and geometric information of each target is corrected by the second measurement dataset $\mathbf{z}_{\mathrm{T}}$, which is obtained from the target detection results on the radar image. The relative bearing and range of a detected target is used to update the vehicle's motion information including position, course, and speed; length measurement is used to update the geometric parameter of the target. The associated equation for the second measurement dataset is expressed as

$$\mathbf{z}_{\mathrm{T}} = \begin{bmatrix} z_\beta \\ z_\rho \\ z_l \end{bmatrix} = \begin{bmatrix} \mathrm{atan}\left(\frac{y_{\mathrm{T}}-y_{\mathrm{U}}}{x_{\mathrm{T}}-x_{\mathrm{U}}}\right) - \psi_{\mathrm{U}} \\ \sqrt{(x_{\mathrm{T}}-x_{\mathrm{U}})^2+(y_{\mathrm{T}}-y_{\mathrm{U}})^2} \\ l_{\mathrm{T}} \end{bmatrix} + \mathbf{v}_{\mathrm{T}} \quad (7)$$

where z_β, z_ρ, and z_l represent the relative bearing, range, and length measurements, respectively. $\mathbf{v}_{\mathrm{T}}$ is the zero-mean Gaussian measurement noise reflecting the uncertainty in the measurement model.

A cell (or blob) on the radar image is defined by the bearing and range resolutions as shown in Fig. 2(a), and multiple cells are occupied by the reflections from a single target. The relative bearing and range measurements are directly obtained from a set of the collected cells; their uncertainties are defined by the span size in the bearing and range directions as shown in Fig. 2(a). On the other hand, the length measurement is not directly extracted from the radar image, and thus an additional procedure is required to extract the length and estimate its associated uncertainty. The length can be obtained from the polygon including radar reflections and the motion state (i.e., target course). To be more specific, as shown in Fig. 2(b), the distance of the intersection points between the boundary of the polygon and the straight line which passes the center of the polygon and has orientation with the angle of the target course defined in the body-fixed frame could be regarded as the length measurement. The uncertainty of the extracted length should be considered for accurate geometric parameter estimation. In this study, the uncertainty is assessed by a finite set of statistics on the extracted multiple length values which are obtained as a function of the target course. As described in Fig. 2(b), the measurement is defined by the course of the target ship and the radar reflections depicted by the fan-shaped polygon; therefore, its value is provided in a nonlinear transformation as a function of the course. The target's course defined in the body-fixed frame is denoted as ψ_{T}^{b} and the associated equation can be written as

$$\psi_{\mathrm{T}}^{b} = \psi_{\mathrm{T}} - \psi_{\mathrm{U}}. \quad (8)$$

The estimated courses of the USV and the target ship follow Gaussian distribution, and thus the equation of the variance of the target's course in the body-fixed frame can be written as

$$\sigma^2_{\psi_{\mathrm{T}}^{b}} = \sigma^2_{\psi_{\mathrm{T}}} + \sigma^2_{\psi_{\mathrm{U}}} - 2\sigma_{\psi_{\mathrm{T}}\psi_{\mathrm{U}}} \quad (9)$$

where $\sigma_{\psi_{\mathrm{T}}}$ and $\sigma_{\psi_{\mathrm{U}}}$ represent the estimated standard deviation of the course angles of the target and the USV, respectively. $\sigma_{\psi_{\mathrm{T}}\psi_{\mathrm{U}}}$ represents the correlation between the course angles.

Considering the nonlinear relation between course ψ_{T}^{b} and length l_{T}, an unscented transform (UT) is employed in this study [32]. To define a discrete distribution from sample data, a set of sigma points of the course is selected; the associated equation is written as

$$\begin{aligned}
\chi_{\psi_{\mathrm{T}}^{b}}^{[0]} &= \mu_{\psi_{\mathrm{T}}^{b}} \\
\chi_{\psi_{\mathrm{T}}^{b}}^{[i]} &= \mu_{\psi_{\mathrm{T}}^{b}} + \sqrt{(n+\lambda)\sigma_{\psi_{\mathrm{T}}^{b}}^{2}}, \quad for\ i = 1, \cdots, n \\
\chi_{\psi_{\mathrm{T}}^{b}}^{[i]} &= \mu_{\psi_{\mathrm{T}}^{b}} - \sqrt{(n+\lambda)\sigma_{\psi_{\mathrm{T}}^{b}}^{2}}, \quad for\ i = n+1, \cdots, 2n
\end{aligned} \tag{10}$$

where $\chi_{\psi_{\mathrm{T}}^{b}}$ and $\mu_{\psi_{\mathrm{T}}^{b}}$ represent the sigma point and mean value of the course of the target in the body-fixed frame, respectively. n is the dimension of the state and λ is a scaling factor whose equation can be written as

$$\lambda = \alpha^2(n+k) - n \tag{11}$$

where α and k are scale parameters that determine the separation spacing of the sigma points from the mean. Among the motion states in the filter, this study assumes that the geometric parameter is only associated with the course state. To estimate the Gaussian distribution of the transformed sigma points in a nonlinear function, the weigh parameters are defined as

$$\begin{aligned}
\omega_m^{[0]} &= \frac{\lambda}{n+\lambda} \\
\omega_c^{[0]} &= \omega_m^{[0]} + (1 - \alpha^2 + \beta) \\
\omega_m^{[i]} &= \omega_c^{[i]} = \frac{1}{2(n+\lambda)}
\end{aligned} \tag{12}$$

where ω_m and ω_c represent the weights for the mean and variance, respectively. β is a user parameter to include additional information related to the distribution underlying the Gaussian representation. From the obtained sigma points and weights, the mean $\mu_{l_{\mathrm{T}}}$ and variance $\sigma_{l_{\mathrm{T}}}^2$ of the transformed state in the nonlinear function are defined respectively as

$$\begin{aligned}
\mu_{l_{\mathrm{T}}} &= \sum_{i=0}^{2n} \omega_m^{[i]} g(\chi_{\psi_{\mathrm{T}}^{b}}^{[i]}) \\
\sigma_{l_{\mathrm{T}}}^2 &= \sum_{i=0}^{2n} \omega_c^{[i]} (g(\chi_{\psi_{\mathrm{T}}^{b}}^{[i]}) - \mu_{l_{\mathrm{T}}})(g(\chi_{\psi_{\mathrm{T}}^{b}}^{[i]}) - \mu_{l_{\mathrm{T}}})^{\mathrm{T}}
\end{aligned} \tag{13}$$

where $g(\chi_{\psi_{\mathrm{T}}^{b}}^{[i]})$ represents the nonlinear mapping function to obtain the length from the i^{th} sigma point of the target course. The mean $\mu_{l_{\mathrm{T}}}$ and variance $\sigma_{l_{\mathrm{T}}}^2$ are applied as the length measurement and its uncertainty, respectively, in the tracking filter.

To associate the newly detected target measurements with the existing target in the filter state, the data association method based on the global nearest neighbor (GNN) is applied [33]. To assign measurements to the corresponding track, a thresholding value is required to evaluate the similarity; an ellipsoidal gate is applied in this study [34]. The equation of the ellipsoidal gate can be written as

$$d^2 = \tilde{\mathbf{z}}^{\top} S^{-1} \tilde{\mathbf{z}} \tag{14}$$

where S and d^2 are the innovation covariance matrix of measurement and the normalized statistical distance, respectively. $\tilde{\mathbf{z}}$ denotes the innovation vector characterized by the discrepancy between the actual and expected measurements. In addition to the difference in position, the length parameter is also considered for reliable and robust data association by estimating the correspondence in a high-dimensional space.

TABLE 1. Specifications of Aragon USV.

Item	Specification
Dimension (LxB)	8.0 m x 2.3 m
Weight	3,000 kg
Maximum speed	> 43 knots
Propulsion	Diesel engine (single waterjet)
Power	440 hp
Operating hours	< 15 hr (per refuel)
Navigation sensors	Radars, IMU, RTK-GPS, GPS compass

TABLE 2. Specifications of onboard pulse radar.

Item	Specification*
Radar model	Furuno FAR-2117
Operating frequency	9,410 ± 30 MHz
Range scale	6 NM
Scanner rotation period	1.7 s
Range resolution ($\Delta\rho$)	11 m
Bearing resolution ($\Delta\beta$)	1.9°
Beamwidth (vertical)	20°
Pulse repetition frequency	914 Hz
Output power	12 kW

∗ The actual performance could differ depending on the operation conditions.

IV. FIELD EXPERIMENTS

Field experiments were conducted to demonstrate the feasibility of the proposed target tracking algorithm using Aragon USV system developed by the Korea Research Institute of Ships and Ocean Engineering (KRISO).

A. USV SYSTEM AND EXPERIMENTAL SETUP

The USV platform is based on a planning hull with a length of 8.0 m, and it is integrated with a waterjet propulsion system. The specifications of the USV system are listed in Table 1. The USV system has various navigation sensors such as real-time kinematic global positioning system (RTK-GPS), GPS compass, IMU, and X-band marine radar as shown in Fig. 3(a). The Furuno pulse radar (FAR-2117) was used for automatic target detection; the sensor specifications are listed in Table 2.

(a) Aragon USV

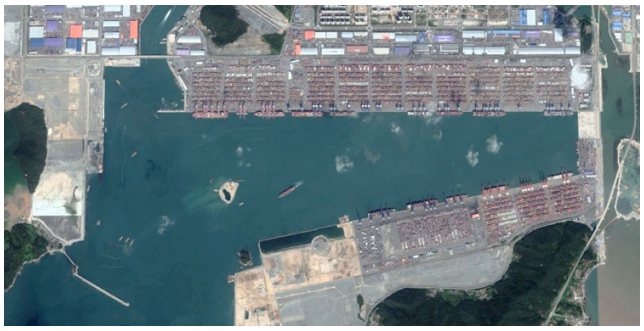

(b) Experimental site

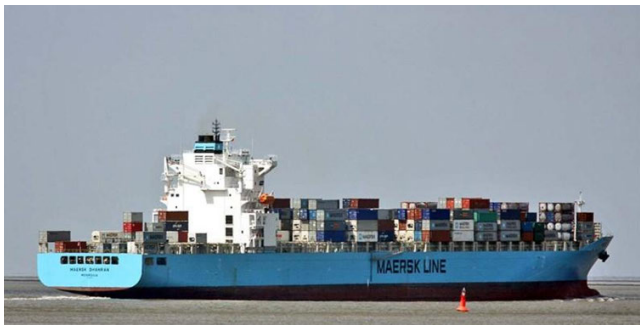

(c) Target ship

FIGURE 3. Experimental setup. (a) Aragon USV system (8.0 m in length). (b) Aerial map of the experimental site near the Pusan Newport International Terminal in the southern Korean sea. (c) MAERSK container ship with a length of 294 m and a breadth of 32 m [35].

The field experiments were performed in the coastal area near Pusan Newport International Terminal in the southern Korean sea, where large commercial ships regularly enter and leave, as shown in Fig. 3(b). During the field test, a large container ship (see Fig. 3(c)) was entering the port and the USV ran in the coastal areas to detect and track the target ship using the onboard pulse radar. AIS data of the target were available, and thus, they were used as ground truth data to evaluate the performance of the proposed target tracking algorithm. The specifications of the target ship are listed in Table 3.

B. RESULTS AND DISCUSSIONS

During the USV operation, the motion states and geometric parameter of the target ship are estimated; the results are shown in Fig. 4.

TABLE 3. Specifications of target ship [35].

Item	Specification
Dimension (LxB)	294.1 m x 32.29 m
MMSI*	636091610
Vessel-type	Cargo (container ship)
Deadweight tonnage	68,578 ton
Gross tonnage	54,675 ton

∗ Maritime mobile service identity

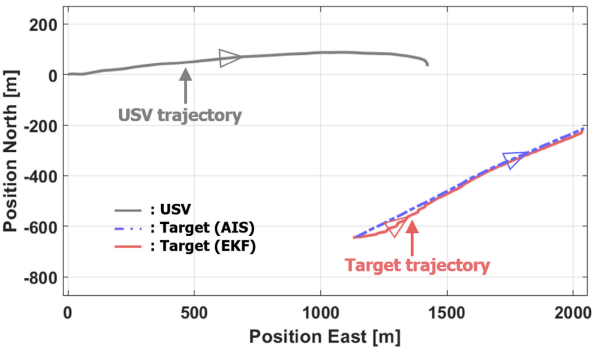

(a) Trajectory

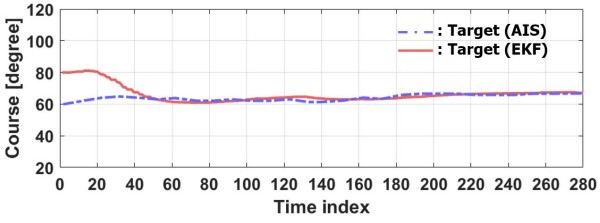

(b) Course

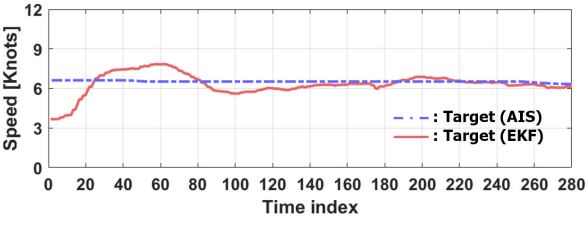

(c) Speed

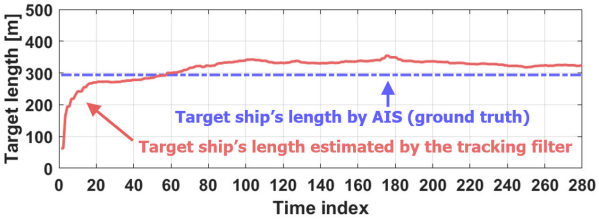

(d) Length

FIGURE 4. Experimental results of the proposed target tracking. (a) Estimated trajectories of the USV and target ship. The triangles represent the direction of the vehicles' motion (not to scale). (b) Estimated course information of the target ship. (c) Estimated speed information of the target ship. (d) Estimated length of the target ship.

The estimated trajectories are compared in Fig. 4(a). The USV trajectory is represented by a solid line in black and the target trajectory estimated by the tracking filter is

represented by a solid line in red. To evaluate the performance of the proposed algorithm, the target's trajectory obtained from AIS data is also represented by a dash-dotted line in blue. From the start point to the goal point, the estimated target trajectory follows the ground-truth data well, thereby confirming the performance of the tracking algorithm for motion estimation.

In addition to the trajectory of the vehicle, the course and speed of the target were estimated in the tracking filter. In Fig. 4(b) and (c), the estimated course and speed are represented by a solid line in red, and the corresponding AIS data are represented by a dash-dotted line in blue. The motion information estimated by the tracking filter successfully converges to the ground-truth data by updating the motion states using radar measurements.

In the tracking filter, the geometric parameter of the target ship was also estimated. In Fig. 4(d), the time history of the estimated geometric parameter is represented by a solid line in red, and the corresponding AIS data are represented by a dash-dotted line in blue. The geometric parameter is initially unknown, and therefore, the initial geometric parameter is set with a length of 80 m in the track initiation process; the parameter is updated with the following radar measurements. According to the AIS data, the actual length of the target ship is 294 m; the estimated length obtained by the proposed tracking filter converges well to near the actual value with satisfactory accuracy.

V. CONCLUSION

This study presented a systematic procedure and associated algorithm for target tracking with a marine radar mounted on a USV. The relative bearing and range measurements were obtained from radar measurements, and then the motion states of the target ship were estimated within the framework of an EKF-based tracking filter. An enhanced target ship tracking approach was proposed to estimate the kinematic and geometric parameters simultaneously.

To evaluate and demonstrate the feasibility of the proposed target tracking algorithm, field experiments were conducted in real-sea environments using Aragon USV developed by KRISO. A container ship with a length of 294 m was detected from pulse radar measurements, and motion states and length of the target ship were estimated and compared with her AIS data (or ground-truth data). The results demonstrate the satisfactory performance and feasibility of the proposed target tracking algorithm.

Collision risk evaluation and automatic collision avoidance are important for the autonomous navigation of USVs. The introduced algorithm can be employed to achieve safe USV operation when AIS data of surrounding traffic ships are not available. From the conducted field experiments, we found out some limitations of the proposed tracking method. In the tracking filter, a constant velocity model is applied, and thus the modeling error driven by the dynamic factors of maneuvering targets may not be effectively reduced by radar measurements due to the relatively slow sampling rate of the radar. Also, the performance of geometric parameter estimation is dependent on sensor resolution characteristics, particularly on the bearing resolution. On a radar image, the span size of a single cell reflected by a target is defined by the relative range and the bearing resolution. Therefore, to further improve performance, a marine radar with a higher resolution or a sensor fusion technique with detection sensors with a high sampling rate should be considered in future research.

REFERENCES

[1] Z. Liu, Y. Zhang, X. Yu, and C. Yuan, "Unmanned surface vehicles: An overview of developments and challenges," *Annu. Rev. Control*, vol. 41, pp. 71–93, Jan. 2016.

[2] Z. Pietrzykowski and J. Uriasz, "The ship domain-a criterion of navigational safety assessment in an open sea area," *J. Navigat.*, vol. 62, no. 1, p. 93, 2009.

[3] J. Park and J. Kim, "Predictive evaluation of ship collision risk using the concept of probability flow," *IEEE J. Ocean. Eng.*, vol. 42, no. 4, pp. 836–845, Oct. 2017.

[4] A. Harati-Mokhtari, A. Wall, P. Brooks, and J. Wang, "Automatic identification system (AIS): Data reliability and human error implications," *J. Navigat.*, vol. 60, no. 3, p. 373, 2007.

[5] L. Malarky and B. Lowell. *Avoiding Detection: Global Case Studies of Possible AIS Avoidance*. Oceana. Accessed: 2018. [Online]. Available: https://usa.oceana.org/publications/reports/avoiding-detection-global-case-studies-possible-ais-avoidance

[6] J. Kim, S. Vaddi, P. Menon, and E. Ohlmeyer, "Comparison between three spiraling ballistic missile state estimators," in *Proc. AIAA Guid., Navigat. Control Conf. Exhib.*, Aug. 2008, p. 7459.

[7] E. W. Frew and S. M. Rock, "Trajectory generation for constant velocity target motion estimation using monocular vision," in *Proc. IEEE Int. Conf. Robot. Autom.*, Sep. 2003, pp. 3479–3484.

[8] Y. Bar-Shalom, X. R. Li, and T. Kirubarajan, *Estimation With Applications to Tracking and Navigation: Theory Algorithms and Software*. Hoboken, NJ, USA: Wiley, 2004.

[9] A. Farina, "Target tracking with bearings–only measurements," *Signal Process.*, vol. 78, no. 1, pp. 61–78, Oct. 1999.

[10] J. Han, Y. Cho, J. Kim, J. Kim, N. Son, and S. Y. Kim, "Autonomous collision detection and avoidance for ARAGON USV: Development and field tests," *J. Field Robot.*, vol. 37, no. 6, pp. 987–1002, Sep. 2020.

[11] S. Blackman and R. Popoli, *Design and Analysis of Modern Tracking Systems*. Norwood, MA, USA: Artech House, 1999.

[12] S. Sato, M. Hashimoto, M. Takita, K. Takagi, and T. Ogawa, "Multilayer lidar-based pedestrian tracking in urban environments," in *Proc. IEEE Intell. Vehicles Symp.*, Jun. 2010, pp. 849–854.

[13] D. Meissner, S. Reuter, and K. Dietmayer, "Real-time detection and tracking of pedestrians at intersections using a network of laserscanners," in *Proc. IEEE Intell. Vehicles Symp.*, Jun. 2012, pp. 630–635.

[14] R. Karlsson and F. Gustafsson, "Recursive Bayesian estimation: Bearings-only applications," *IEE Proc. Radar, Sonar Navigat.*, vol. 152, no. 5, pp. 305–313, Oct. 2005.

[15] J. Kim, T. Suh, and J. Ryu, "Bearings-only target motion analysis of a highly manoeuvring target," *IET Radar, Sonar Navigat.*, vol. 11, no. 6, pp. 1011–1019, Jun. 2017.

[16] Y.-S. Kim and K.-S. Hong, "An IMM algorithm for tracking maneuvering vehicles in an adaptive cruise control environment," *Int. J. Control, Autom., Syst.*, vol. 2, no. 3, pp. 310–318, 2004.

[17] G. Vivone, P. Braca, K. Granström, A. Natale, and J. Chanussot, "Converted measurements Bayesian extended target tracking applied to X-band marine radar data," NATO Sci. Technol. Org., La Spezia, Italy, Tech. Rep. CMRE-PR-2019-076, 2019.

[18] K. Granström, A. Natale, P. Braca, G. Ludeno, and F. Serafino, "Gamma Gaussian inverse wishart probability hypothesis density for extended target tracking using X-band marine radar data," *IEEE Trans. Geosci. Remote Sens.*, vol. 53, no. 12, pp. 6617–6631, Dec. 2015.

[19] G. Vivone, P. Braca, K. Granstrom, and P. Willett, "Multistatic Bayesian extended target tracking," *IEEE Trans. Aerosp. Electron. Syst.*, vol. 52, no. 6, pp. 2626–2643, Dec. 2016.

[20] K. Granström, A. Natale, P. Braca, G. Ludeno, and F. Serafino, "PHD extended target tracking using an incoherent X-band radar: Preliminary real-world experimental results," in *Proc. 17th Int. Conf. Inf. Fusion (FUSION)*, 2014, pp. 1–8.
[21] O. E. Drummond, "Tracking clusters and extended objects with multiple sensors," in *Proc. Signal Data Process. Small Targets*, vol. 1305, Oct. 1990, p. 362.
[22] O. Drummond, S. Blackman, and K. Hell, "Multiple sensor tracking of clusters and extended objects," in *Proc. Tech. Tri-Service Data Fusion Symp.*, 1988, pp. 231–238.
[23] G. Vivone and P. Braca, "Joint probabilistic data association tracker for extended target tracking applied to X-band marine radar data," *IEEE J. Ocean. Eng.*, vol. 41, no. 4, pp. 1007–1019, Oct. 2016.
[24] K. Granstrom, M. Baum, and S. Reuter, "Extended object tracking: Introduction, overview and applications," 2016, *arXiv:1604.00970*. [Online]. Available: http://arxiv.org/abs/1604.00970
[25] G. Vivone, P. Braca, and B. Errasti-Alcala, "Extended target tracking applied to X-band marine radar data," in *Proc. OCEANS Genova*, May 2015, pp. 1–6.
[26] K. Granström, C. Lundquist, and U. Orguner, "Tracking rectangular and elliptical extended targets using laser measurements," in *Proc. 14th Int. Conf. Inf. Fusion*, 2011, pp. 1–8.
[27] K. Granström, S. Reuter, D. Meissner, and A. Scheel, "A multiple model PHD approach to tracking of cars under an assumed rectangular shape," in *Proc. 17th Int. Conf. Inf. Fusion (FUSION)*, 2014, pp. 1–8.
[28] A. Petrovskaya and S. Thrun, "Model based vehicle tracking for autonomous driving in urban environments," in *Proc. Robot., Sci. Syst.* Zurich, Switzerland, vol. 34, Jun. 2008, pp. 1–8.
[29] J. Han, N.-S. Son, and J. Kim, "Automatic target tracking with time-delayed measurements for unmanned surface vehicles," in *Proc. SPIE Future Sens. Technol.*, Nov. 2019, Art. no. 111971B.
[30] Cambridge Pixel Ltd. *SPx Development Library*. Accessed: Mar. 20, 2020. [Online]. Available: http://www.cambridgepixel.com
[31] H. Rohling, "Radar CFAR thresholding in clutter and multiple target situations," *IEEE Trans. Aerosp. Electron. Syst.*, vol. AES-19, no. 4, pp. 608–621, Jul. 1983.
[32] S. Thrun, W. Burgard, and D. Fox, *Probabilistic Robotics*, vol. 1. Cambridge, MA, USA: MIT Press, 2000.
[33] S. Blackman and R. Popoli, *Design and Analysis of Modern Tracking Systems (Book)*. Norwood, MA, USA: Artech House, 1999.
[34] Y. Zhu, J. Wang, S. Liang, and J. Wang, "Covariance control joint integrated probabilistic data association filter for multi-target tracking," *IET Radar, Sonar Navigat.*, vol. 13, no. 4, pp. 584–592, Apr. 2019.
[35] *PixelOpa*. [Online]. Available: http://www.marinetraffic.com

JUNGWOOK HAN received the B.S. degree in mechanical engineering from Ajou University, Suwon, South Korea, in 2009, and the M.S. degree in ocean systems engineering and the Ph.D. degree in mechanical engineering from Korea Advanced Institute of Science and Technology, Daejeon, South Korea, in 2013 and 2019, respectively. He was selected as a Scholarship Student of the IEEE OES Scholarship Program, in 2016. He is currently a Senior Researcher with the Korea Research Institute of Ships and Ocean Engineering, Daejeon. His research interests include the areas of USV navigation, 3D reconstruction, multi-sensor target tracking, and SLAM.

SUN YOUNG KIM received the B.S. and M.S. degrees with the Department of Naval Architecture and Ocean Engineering, Seoul National University, South Korea, in 1983 and 1985, respectively, and the Ph.D. degree from Hiroshima University, Japan, in 1993. He is a Principal Researcher with the Autonomous and Intelligent Maritime Systems Research Division, Korea Research Institute of Ships and Ocean Engineering (KRISO). Since 1985, he has been working for ship maneuvering and maritime safety at KRISO. His research interests include USV development and safety of navigation.

JINWHAN KIM (Member, IEEE) received the B.S. and M.S. degrees in naval architecture and ocean engineering from Seoul National University, South Korea, and the Ph.D. degree in aeronautics and astronautics and the Ph.D. degree in electrical engineering from Stanford University. He was with the Korea Institute of Machinery and Materials and the Korea Ocean Research and Development Institute, as a full-time Researcher. In 2010, he joined the Faculty of Mechanical Engineering, Korea Advanced Institute of Science and Technology (KAIST), where has been working in the areas of vehicle guidance, navigation, control, and marine robotics. He is currently a Senior Member of AIAA.